

Introduction

The supplementary material describes the governing equations and the parameter settings of the CoSiNE model. Supplementary figures are also provided in this document.

Text S1. Governing equations of the CoSiNE-Fe model

The equations describing individual compartments in the model all take the following form:

$$\frac{\partial B_i}{\partial t} = PHY(B_i) + BIO(B_i).$$

where $PHY(B_i)$ represents the contribution to concentration change from physical processes. $BIO(B_i)$ represents biological source/sink of a particular compartment. The model state variable (Table S1), B_i , represents small phytoplankton (S1 (mmol N m^{-3}), Chl1 (mg m^{-3}), S1Fe ($\mu\text{mol Fe m}^{-3}$)), diatom (S2 (mmol N m^{-3}), Chl2 (mg m^{-3}), S2Fe ($\mu\text{mol Fe m}^{-3}$)), microzooplankton (zz1 (mmol N m^{-3}), zz1Fe ($\mu\text{mol Fe m}^{-3}$)), mesozooplankton (zz2 (mmol N m^{-3}), zz2Fe ($\mu\text{mol Fe m}^{-3}$)), large detritus (LPON (mmol N m^{-3}), LPFe ($\mu\text{mol Fe m}^{-3}$)), small detritus (SPON (mmol N m^{-3}), SPFe ($\mu\text{mol Fe m}^{-3}$)), large biogenic silica (LbSi (mmol Si m^{-3})), small biogenic silica (SbSi (mmol Si m^{-3})), nitrate (NO3 (mmol N m^{-3})), ammonium (NH4 (mmol N m^{-3})), phosphate (PO4 (mmol P m^{-3})), silicate (SiOH4 (mmol Si m^{-3})), dissolved oxygen (DO (mmol m^{-3})), total alkalinity (TALK (mmol m^{-3})), dissolved inorganic carbon (DIC (mmol C m^{-3})), dust particles (PartDust (mg m^{-3}), DustFe ($\mu\text{mol Fe m}^{-3}$)), large lithogenic particles (LithPartL (mg m^{-3}), LithLFe ($\mu\text{mol Fe m}^{-3}$)), small lithogenic particles (LithPartS (mg m^{-3}), LithSFe ($\mu\text{mol Fe m}^{-3}$)), colloidal Fe (FeCol ($\mu\text{mol Fe m}^{-3}$)), soluble Fe (FeSol ($\mu\text{mol Fe m}^{-3}$)), strong ligand Fe (FeLgS ($\mu\text{mol Fe m}^{-3}$)), weak ligand Fe (FeLgW ($\mu\text{mol Fe m}^{-3}$)), strong ligands (LgS ($\mu\text{mol m}^{-3}$)), and weak ligands (LgW ($\mu\text{mol m}^{-3}$)).

Table S1. Model state variable and corresponding abbreviations in model equation

Model state variable	Abbreviations
small phytoplankton (mmol N m^{-3})	S1
chlorophyll <i>a</i> of small phytoplankton (mg m^{-3})	Chl1
Fe of small phytoplankton ($\mu\text{mol Fe m}^{-3}$)	S1Fe
diatom (mmol N m^{-3})	S2
chlorophyll <i>a</i> of diatom (mg m^{-3})	Chl2
Fe of diatom ($\mu\text{mol Fe m}^{-3}$)	S2Fe
microzooplankton (mmol N m^{-3})	zz1
Fe of microzooplankton ($\mu\text{mol Fe m}^{-3}$)	zz1Fe
mesozooplankton (mmol N m^{-3})	zz2

Fe of mesozooplankton ($\mu\text{mol Fe m}^{-3}$)	zz2Fe
large detritus (mmol N m^{-3})	LPON
Fe of large detritus ($\mu\text{mol Fe m}^{-3}$)	LPFe
small detritus (mmol N m^{-3})	SPON
Fe of small detritus ($\mu\text{mol Fe m}^{-3}$)	SPFe
large biogenic silica (mmol Si m^{-3})	LbSi
small biogenic silica (mmol Si m^{-3}),	SbSi
nitrate (mmol N m^{-3})	NO3
ammonium (mmol N m^{-3})	NH4
phosphate (mmol P m^{-3})	PO4
silicate (mmol Si m^{-3})	SiOH4
dissolved oxygen (mmol m^{-3})	DO
total alkalinity (mmol m^{-3})	TALK
dissolved inorganic carbon (mmol C m^{-3})	DIC
dust particles (mg m^{-3})	PartDust
Fe of dust particles ($\mu\text{mol Fe m}^{-3}$)	DustFe
large lithogenic particles (mg m^{-3})	LithPartL
Fe of large lithogenic particles ($\mu\text{mol Fe m}^{-3}$)	LithLFe
small lithogenic particles (mg m^{-3})	LithPartS
Fe of small lithogenic particles ($\mu\text{mol Fe m}^{-3}$)	LithSFe
colloidal Fe ($\mu\text{mol Fe m}^{-3}$)	FeCol
soluble Fe ($\mu\text{mol Fe m}^{-3}$)	FeSol
strong ligand Fe ($\mu\text{mol Fe m}^{-3}$)	FeLgS
weak ligand Fe ($\mu\text{mol Fe m}^{-3}$)	FeLgW
strong ligands ($\mu\text{mol m}^{-3}$)	LgS
weak ligands ($\mu\text{mol m}^{-3}$)	LgW

Biological processes controlling changes in phytoplankton, zooplankton, inorganic nutrients, dissolved oxygen, total alkalinity, and dissolved inorganic carbon are from the CoSiNE model, which were described in Ma et al. (2019). The equations related to the dynamics of different particles and the Fe cycle were obtained from Xiu & Chai (2021). Here, we only show equations related to the dynamics of different particles and the Fe cycle.

$$\begin{aligned}
 \text{BIO(PartDust)} &= \text{Fluxdust} - \text{atmospheric deposition} - \text{dustcoag1} - \text{coagulation} - \text{dustcoag4} - \text{coagulation} - w_{dust} \frac{\partial \text{Partdust}}{\partial z} \\
 \text{BIO(LithPartS)} &= \text{dustcoag1} - \text{coagulation} - \text{dustcoag3} - \text{coagulation} - \text{dustcoag2} - \text{coagulation} - w_{sd} \frac{\partial \text{LithPartS}}{\partial z} \\
 \text{BIO(LithPartL)} &= \text{dustcoag4} + \text{coagulation} + \text{dustcoag3} + \text{coagulation} + \text{dustcoag2} - \text{coagulation} - w_{sd2} \frac{\partial \text{LithPartL}}{\partial z} \\
 \text{BIO(DustFe)} &= k_{sca} \times \text{FeSol} \times \text{PartDust} + k_{ag} \times \text{FeCol} \times \text{PartDust} - \text{dustFecoag1} \\
 &\quad \text{soluble iron scavenging} \quad \text{colloidal iron aggregation} \quad \text{coagulation} \quad \text{coagulation} \\
 &\quad - fpar \times k_{ph4} \times \text{DustFe} - k_{pd} \times \text{DustFe} - \text{dustFecoag4} - w_{dust} \frac{\partial \text{Fedust}}{\partial z} \\
 \text{BIO(LithSFe)} &= k_{sca} \times \text{FeSol} \times (\text{SPON} \times \text{rmn} + \text{LithPartS}) \\
 &\quad \text{soluble iron scavenging} \\
 &\quad + k_{ag} \times \text{FeCol} \times (\text{SPON} \times \text{rmn} + \text{LithPartS}) + \text{dustFecoag1} - \text{dustFecoag3} \\
 &\quad \text{colloidal iron aggregation} \quad \text{coagulation} \quad \text{coagulation} \quad \frac{\partial \text{LithSFe}}{\partial z} \\
 &\quad - \text{dustFecoag2} - fpar \times k_{ph4} \times \text{LithSFe} - k_{pd} \times \text{LithSFe} - w_{sd} \frac{\partial \text{LithSFe}}{\partial z} \\
 \text{BIO(LithLFe)} &= k_{sca} \times \text{FeSol} \times (\text{LPON} \times \text{rmn} + \text{LithPartL}) \\
 &\quad \text{soluble iron scavenging} \\
 &\quad + k_{ag} \times \text{FeCol} \times (\text{LPON} \times \text{rmn} + \text{LithPartL}) + \text{dustFecoag4} + \text{dustFecoag2} \\
 &\quad \text{colloidal iron aggregation} \quad \text{coagulation} \quad \text{coagulation} \quad \frac{\partial \text{LithLFe}}{\partial z} \\
 &\quad + \text{dustFecpag3} - fpar \times k_{ph4} \times \text{LithLFe} - k_{pd} \times \text{LithLFe} - w_{sd2} \frac{\partial \text{LithLFe}}{\partial z} \\
 \text{BIO(FeCol)} &= k_{pd} \times (\text{DustFe} + \text{LithSFe} + \text{LithLFe}) + k_{col} \times \text{FeSol} \\
 &\quad \text{redissolution} \quad \text{colloidal iron formation} \\
 &\quad - k_{ag} \times \text{FeCol} \times (\text{PartDust} + \text{LithPartS} + \text{LithPartL} + (\text{SPON} + \text{LPON}) \times \text{rmn}) \\
 &\quad \text{aggregation} \\
 &\quad - k_{cd} \times \text{FeCol} - fpar \times k_{ph1} \times \text{FeCol} \\
 &\quad \text{redissolution} \quad \text{photoreduction} \\
 \text{BIO(FeSol)} &= \text{FluxFeSol} + k_{cd} \times \text{FeCol} + k_{flwd} \times \text{FeLgW} + k_{flsd} \times \text{FeLgS} \\
 &\quad \text{atmospheric deposition} \quad \text{colloidal iron redissolution} \quad \text{ligand iron dissociation} \quad \text{ligand iron dissociation} \\
 &\quad - k_{sca} \times \text{FeSol} \times (\text{PartDust} + \text{LithPartS} + \text{LithPartL} + (\text{SPON} + \text{LPON}) \times \text{rmn}) \\
 &\quad \text{scavenging} \\
 &\quad + fpar \times k_{ph4} \times (\text{DustFe} + \text{FelithS} + \text{FelithL}) + fpar \times k_{ph1} \times \text{FeCol} \\
 &\quad \text{photoreduction} \quad \text{photoreduction} \\
 &\quad + fpar \times k_{phls} \times \text{FeLgS} + fpar \times k_{phlw} \times \text{FeLgW} - k_{col} \times \text{FeSol} \\
 &\quad \text{photoreduction} \quad \text{photoreduction} \quad \text{colloidal iron formation} \\
 &\quad - k_{fel} \times \text{FeSol} \times (\text{LgW} + \text{LgS}) - \text{uptakeFeSol1} - \text{uptakeFeSol2} \\
 &\quad \text{ligand iron formation} \quad \text{uptake by S1} \quad \text{uptake by S2} \\
 \text{BIO(FeLgS)} &= k_{fel} \times \text{FeSol} \times \text{LgS} - k_{flsd} \times \text{FeLgS} - fpar \times k_{phls} \times \text{FeLgS} \\
 &\quad \text{ligand iron formation} \quad \text{ligand iron dissociation} \quad \text{photoreduction} \\
 &\quad - \text{uptakeFeLgS1} - \text{uptakeFeLgS2} \\
 &\quad \text{uptake by S1} \quad \text{uptake by S2} \\
 \text{BIO(FeLgW)} &= k_{fel} \times \text{FeSol} \times \text{LgW} - k_{flwd} \times \text{FeLgW} - fpar \times k_{phlw} \times \text{FeLgW} \\
 &\quad \text{ligand iron formation} \quad \text{ligand iron dissociation} \quad \text{photoreduction} \\
 &\quad + (\gamma_5 \times \text{SPFe} + \text{rmiLPFe} + \gamma_3 \times \text{S1Fe} + \gamma_4 \times \text{S2Fe} + \text{reg}_1 \times \text{zz1Fe} \\
 &\quad \text{ligand iron production} \\
 &\quad + \text{reg}_2 \times \text{zz2Fe}) - \text{uptakeFeLgW1} - \text{uptakeFeLgW2} \\
 &\quad \text{uptake by S1} \quad \text{uptake by S2}
 \end{aligned}$$

$$\begin{aligned}
 \text{BIO(LgS)} &= f_{\gamma p1} \times \text{fqfunc1} \times S1 + f_{\gamma p2} \times \text{ffunc2} \times S2 + k_{flsd} \times \text{FeLgS} \\
 &\quad - k_{fel} \times \text{FeSol} \times \text{Lgst} - k_{\gamma ls} \times \text{LgS} \\
 &\quad \text{production by S1} \quad \text{production by S2} \quad \text{ligand iron dissociation} \\
 &\quad \text{ligand iron formation} \quad \text{remineralization} \\
 \text{BIO(LgW)} &= f_{\gamma d1} \times (\text{SPON} + \text{LPON}) + k_{flwd} \times \text{FeLgW} + f_{par} \times k_{phls} \times \text{FeLgS} \\
 &\quad - k_{fel} \times \text{FeSol} \times \text{LgW} - k_{\gamma lw} \times \text{LgW} \\
 &\quad \text{production} \quad \text{ligand iron dissociation} \quad \text{photoreduction} \\
 &\quad \text{ligand iron formation} \quad \text{remineralization} \\
 \text{BIO(S1Fe)} &= \text{totalironuptake1} - g_{s1fezz1} - \gamma_3 \times S1Fe - a_{ggs1fe} - w_{s1} \frac{\partial S1Fe}{\partial z} \\
 &\quad \text{uptake by S1} \quad \text{grazing} \quad \text{mortality} \quad \text{aggregation} \quad \text{sinking} \\
 \text{BIO(S2Fe)} &= \text{totalironuptake2} - g_{s2fezz2} - \gamma_4 \times S2Fe - a_{ggs2fe} - w_{s2} \frac{\partial S2Fe}{\partial z} \\
 &\quad \text{uptake by S2} \quad \text{grazing} \quad \text{mortality} \quad \text{aggregation} \quad \text{sinking} \\
 \text{BIO(zz1Fe)} &= \gamma_1 \times g_{s1fezz1} - g_{zz1fezz2} - r_{g1} \times zz1Fe - \gamma_{10} \times zz1Fe \\
 &\quad \text{grazing} \quad \text{predation} \quad \text{excretion} \quad \text{mortality} \\
 \text{BIO(zz2Fe)} &= \gamma_2 \times g_{tfezz2} - r_{g2} \times zz2Fe - \gamma_0 \times zz2Fe \times zz2Fe \\
 &\quad \text{grazing} \quad \text{excretion} \quad \text{removal} \\
 \text{BIO(SPFe)} &= (1 - \gamma_1) \times g_{s1fezz1} - g_{SPFezz2} + \gamma_3 \times S1Fe - \gamma_5 \times SPFe + a_{ggs1fe} \\
 &\quad \text{fecal pellet by zz1} \quad \text{grazing by zz2} \quad \text{S1 mortality} \quad \text{remineralization} \quad \text{aggregation} \\
 &\quad + (1 - \gamma_2) \times (g_{SPFezz2} + g_{zz1fezz2} + g_{LPFezz2}) + \gamma_4 \times S2Fe + \gamma_{10} \times zz1Fe \\
 &\quad \text{fecal pellet by zz2} \quad \text{S2 mortality} \quad \text{zz1 mortality} \\
 &\quad + \gamma_0 \times zz2Fe \times zz2Fe - k_{coag2} \times SPFe \times (\text{SPON} \times \text{rmn} + \text{LithPartS}) \\
 &\quad \text{zz2 removal} \quad \text{coagulation} \\
 &\quad - k_{coag3} \times SPFe \times (\text{LPON} \times \text{rmn} + \text{LithPartL}) - w_{sd} \frac{\partial SPFe}{\partial z} \\
 &\quad \text{coagulation} \quad \text{sinking} \\
 \text{BIO(LPFe)} &= (1 - \gamma_2) \times g_{s2fezz2} - g_{LPFezz2} - r_{miLPFe} + a_{ggs2fe} \\
 &\quad \text{fecal pellet} \quad \text{grazing by zz2} \quad \text{remineralization} \quad \text{aggregation} \\
 &\quad + k_{coag2} \times SPFe \times (\text{SPON} \times \text{rmn} + \text{LithPartS}) \\
 &\quad \text{coagulation} \\
 &\quad + k_{coag3} \times SPFe \times (\text{LPON} \times \text{rmn} + \text{LithPartL}) - w_{sd2} \frac{\partial LPFe}{\partial z} \\
 &\quad \text{coagulation} \quad \text{sinking}
 \end{aligned}$$

The processes related to particle coagulations are modeled as follows:

$$f_{par} = \frac{\text{PAR}}{\text{PARref}}$$

$$\text{dustcoag1} = k_{coag1} \times \text{PartDust} \times (\text{SPON} \times \text{rmn} + \text{LithPartS})$$

$$\text{dustcoag4} = k_{coag4} \times \text{PartDust} \times (\text{LPON} \times \text{rmn} + \text{LithPartL})$$

$$\text{dustcoag3} = k_{coag3} \times \text{LithPartS} \times (\text{LPON} \times \text{rmn} + \text{LithPartL})$$

$$\text{dustcoag2} = k_{coag2} \times \text{LithPartS} \times (\text{SPON} \times \text{rmn} + \text{LithPartS})$$

$$\text{dustFecoag1} = k_{coag1} \times \text{DustFe} \times (\text{SPON} \times \text{rmn} + \text{LithPartS})$$

$$\text{dustFecoag4} = k_{coag4} \times \text{DustFe} \times (\text{LPON} \times \text{rmn} + \text{LithPartL})$$

$$\text{dustFecoag3} = k_{coag3} \times \text{LithSFe} \times (\text{LPON} \times \text{rmn} + \text{LithPartL})$$

$$\text{dustFecoag2} = k_{coag2} \times \text{LithSFe} \times (\text{SPON} \times \text{rmn} + \text{LithPartS})$$

Assuming soluble Fe, strong and weak ligands of Fe are all bioavailable, and the Fe uptakes by phytoplankton can be modeled as follows:

$$Q_{FeS1} = S1Fe/S1$$

```

QfeS2 = S2Fe/S2
fqfunc1 = (Qfemax - QfeS1)/Qfemax
fqfunc2 = (Qfemax - QfeS2)/Qfemax
ffeS1 = (QfeS1 - Qfemin)/(Qfemax - Qfemin)
ffeS2 = (QfeS2 - Qfemin)/(Qfemax - Qfemin)
totalironuptake1 = (nps1 + rps1) × Qfemax × (1.0 - ffeS1)/(1.015 - ffeS1)
totalironuptake2 = (nps2 + rps2) × Qfemax × (1.0 - ffeS2)/(1.015 - ffeS2)
bioFe = FeSol + FeLgS + FeLgW
uptakeFeSol1 = totalironuptake1 × FeSol/bioFe
uptakeFeSol2 = totalironuptake2 × FeSol/bioFe
uptakeFeLgW1 = totalironuptake1 × FeLgW/bioFe
uptakeFeLgW2 = totalironuptake2 × FeLgW/bioFe
uptakeFeLgS1 = totalironuptake1 × FeLgS/bioFe
uptakeFeLgS2 = totalironuptake2 × FeLgS/bioFe

```

Processes related to phytoplankton aggregation and zooplankton grazing are modeled as follows:

```

aggs1fe = γ6 × (S1 + S2) × S1Fe
aggs2fe = γ6 × (S1 + S2) × S2Fe
ξ1 = ρ1 × S2 + ρ2 × zz1 + ρ3 × SPON + ρ4 × LPON
ξ2 = ρ1 × S22 + ρ2 × zz12 + ρ3 × SPON2 + ρ4 × LPON2
gs1fezz1 = G1max × zz1 × S1Fe/(akz1 + S1)
gs2fezz2 = G2max × ρ1 × S2 × S2Fe × zz2/(akz2 × ξ1 + ξ2)
gzz1fezz2 = G2max × ρ2 × zz1 × zz1Fe × zz2/(akz2 × ξ1 + ξ2)
gSPFezz2 = G2max × ρ3 × SPON × SPFe × zz2/(akz2 × ξ1 + ξ2)
gLPMFezz2 = G2max × ρ4 × LPON × LPFe × zz2/(akz2 × ξ1 + ξ2)
gtfezz2 = gs2fezz2 + gzz1fezz2 + gSPFezz2 + gLPMFezz2

```

Phytoplankton growth, new production and regenerated production for picoplankton and diatoms are modeled as follows:

```

Q10 = ekt × (T - 10), where T is the water temperature
uno3s1 = e-ψ1NH4 × NO3/(kno3_s1 + NO3)
unh4s1 = NH4/(knh4_s1 + NH4)
upo4s1 = PO4/(kpo4_s1 + PO4)
ufes1 = bioFe/(kfe_s1 + bioFe)
grows1 = min(uno3s1 + unh4s1, upo4s1, uifes1)
nps1 = μ1max × grows1 ×  $\frac{\text{uno3s1}}{\text{uno3s1} + \text{unh4s1}} \times [1 - \exp\left(\frac{-\alpha_{s1}PAR}{\mu1_{max}}\right)] \times S1 \times Q10$ 
rps1 = μ1max × grows1 ×  $\frac{\text{unh4s1}}{\text{uno3s1} + \text{unh4s1}} \times [1 - \exp\left(\frac{-\alpha_{s1}PAR}{\mu1_{max}}\right)] \times S1 \times Q10$ 
uno3s2 = e-ψ2NH4 × NO3/(kno3_s2 + NO3)
unh4s2 = NH4/(knh4_s2 + NH4)
upo4s2 = PO4/(kpo4_s2 + PO4)

```

$$\begin{aligned}
 u_{fes2} &= \text{bioFe}/(k_{fe_s2} + \text{bioFe}) \\
 u_{si04s2} &= \text{SiOH4}/(k_{si_s2} + \text{SiOH4}) \\
 \text{grows2} &= \min(\text{uno3s2} + \text{unh4s2}, \text{upo4s2}, \text{ufes2}, \text{usio4s2}) \\
 nps2 &= \mu_{2max} \times \text{grows2} \times \frac{\text{uno3s2}}{\text{uno3s2} + \text{unh4s2}} \times [1 - \exp\left(\frac{-\alpha_{s2}PAR}{\mu_{2max}}\right)] \times S2 \times Q10 \\
 rps2 &= \mu_{2max} \times \text{grows2} \times \frac{\text{unh4s2}}{\text{uno3s2} + \text{unh4s2}} \times [1 - \exp\left(\frac{-\alpha_{s2}PAR}{\mu_{2max}}\right)] \times S2 \times Q10
 \end{aligned}$$

Table S2. Model parameters

Parameter values for a temperature of 10°C used in the model simulations

Symbols	Descriptions	Values	Units	Source
ψ_1	NH ₄ inhibition for S1	1.5	mmol N m ⁻³	(3), (6)
ψ_2	NH ₄ inhibition for S2	1.5	mmol N m ⁻³	(3), (6)
k_{no3_s1}	Half-saturation for NO ₃ uptake by S1	3.0	mmol N m ⁻³	(3)
k_{nh4_s2}	Half-saturation for NH ₄ uptake by S1	0.3	mmol N m ⁻³	(3)
k_{no3_s2}	Half-saturation for NO ₃ uptake by S2	3.0	mmol N m ⁻³	(3)
k_{nh4_s1}	Half-saturation for NH ₄ uptake by S2	0.3	mmol N m ⁻³	(3)
k_{si_s1}	Half-saturation for SiO ₄ uptake by S2	3.0	mmol Si m ⁻³	(3)
K_{po4_s1}	Half-saturation for PO ₄ uptake by S1	0.02	mmol N m ⁻³	(6)
K_{po4_s2}	Half-saturation for PO ₄ uptake by S2	0.05	mmol Si m ⁻³	(6)
μ_{1max}	Maximum growth rate of S1	2.0	d ⁻¹	(4), (5)
μ_{2max}	Maximum growth rate of S2	3.0	d ⁻¹	(4)
γ_1	Grazing efficiency of Z1	0.95	-	(6)
γ_2	Grazing efficiency of Z2	0.75	-	(4), (6)
γ_3	S1 mortality	0.08	d ⁻¹	(3)
γ_4	S2 mortality	0.01	d ⁻¹	(4)
γ_5	Remineralization rate of PONs	0.1	d ⁻¹	(4)
γ_6	Aggregation rate	0.05	d ⁻¹	this study
γ_7	Nitrification rate	0.1	d ⁻¹	this study
γ_8	Remineralization rate of PON _L	0.5	d ⁻¹	this study
γ_9	Remineralization rate of bSiO ₂	0.5	d ⁻¹	this study
γ_{10}	Loss rate of Z2	0.05	d ⁻¹	(1), (4)
reg1	Excretion rate of Z1	0.1	d ⁻¹	(4)
reg2	Excretion rate of Z2	0.05	d ⁻¹	(4)
α_{s1}	Initial slope of P-I curve of S1	0.025	(W m ⁻²) ⁻¹ d ⁻¹	(1), (4)

α_{s2}	Initial slope of P-I curve of S2	0.025	(W m ⁻²) ⁻¹ d ⁻¹	(1), (4)
G1 _{max}	Maximum grazing rate by Z1	1.3	d ⁻¹	(5)
G2 _{max}	Maximum grazing rate by Z2	0.6	d ⁻¹	this study
ρ_1	Z2 grazing preference for P2	0.70	-	(1), (4)
ρ_2	Z2 grazing preference for Z1	0.20	-	(1), (4)
ρ_3	Z2 grazing preference for PONs	0.03	-	(4)
ρ_4	Z2 grazing preference for PONL	0.07	-	(4)
K1 _{gr}	Half saturation constant for Z1 grazing	0.5	mmol N m ⁻³	(1), (4)
K2 _{gr}	Half saturation constant for Z2 grazing	0.25	mmol N m ⁻³	(1), (4)
W1	Sinking velocity of S1 and Chl1	0.1	m d ⁻¹	(4)
W2	Sinking velocity of S2 and Chl2	0.6	m d ⁻¹	(4)
W3	Sinking velocity of bSiO ₂	60	m d ⁻¹	(4)
W _{sd}	Sinking velocity of PONs	2	m d ⁻¹	(4)
W _{sd2}	Sinking velocity of PONL	40	m d ⁻¹	this study
W _{dust}	Sinking velocity of dust particle	0.1	m d ⁻¹	(6)
R _{PN}	Ratio of P to N	0.0625	mol P/mol N	(1), (4)
R _{CN}	Ratio of C to N	6.625	mol C/mol N	(1), (4)
R _{SiN}	Ratio of Si to N	1.5	mol Si/mol N	(1), (4)
R _{O2NO3}	Ratio of O ₂ to NO ₃	8.625	mol O ₂ /mol NO ₃	(4)
R _{O2NH4}	Ratio of O ₂ to NH ₄	6.625	mol O ₂ /mol NH ₄	(4)
$R_{C,max}^{Chl}$	Maximum ratio of Chl-a to carbon	0.05	-	(4)
k _T	Temperature coefficient for the rate of biological activity	0.0693	°C ⁻¹	(2)
S1 _{Z1}	Threshold value for Z1 grazing S1	0.045	mmol N m ⁻³	(3)
S2 _{Z2}	Threshold value for Z2 grazing S2	0.045	mmol N m ⁻³	(3)
Z1 _{Z2}	Threshold value for Z2 grazing Z1	0.08	mmol N m ⁻³	this study
rmn	Mass:N ratio in organic matter	159	g mol ⁻¹	(6)
Qfemin	Minimum Fe:N ration in organic matter	0.0066	µmol m ⁻³ (mmol m ⁻³) ⁻¹	(6)
Qfemax	Maximum Fe:N ration in organic matter	0.033	µmol m ⁻³ (mmol m ⁻³) ⁻¹	(6)
k _{coag1}	Coagulation rate	0.0003888	m ³ (mg d) ⁻¹	(6)
k _{coag2}	Coagulation rate	0.0009504	m ³ (mg d) ⁻¹	(6)
k _{coag3}	Coagulation rate	0.0013	m ³ (mg d) ⁻¹	(6)
k _{coag4}	Coagulation rate	0.0011	m ³ (mg d) ⁻¹	(6)
K _{sca}	Soluble Fe scavenging rate	0.00015	m ³ (mg d) ⁻¹	(6)
PARref	Reference PAR	400.0	W m ⁻²	(6)
k _{ph1}	Colloidal Fe photoreduction rate	20.2	d ⁻¹	(6)
k _{ph4}	Particulate Fe photoreduction rate	20.2	d ⁻¹	(6)

k_{pd}	Particulate Fe redissolution rate	0.015	d^{-1}	(6)
k_{col}	Colloidal Fe formation rate	2.4	d^{-1}	(6)
k_{cd}	Colloidal Fe redissolution rate	0.41	d^{-1}	(6)
k_{ag}	Colloidal Fe aggregation rate	0.001224	$m^3 (mg\ d)^{-1}$	(6)
k_{flwd}	Weak ligand Fe dissociation rate	8.64	d^{-1}	(6)
k_{flsd}	Strong ligand Fe dissociation rate	0.1	d^{-1}	(6)
k_{fel}	Ligand Fe formation rate	35.0	$(\mu mol\ m^{-3}\ d)^{-1}$	(6)
k_{phls}	Strong ligand Fe photoreduction rate	0.38	d^{-1}	(6)
k_{phlw}	Weak ligand Fe photoreduction rate	7.6	d^{-1}	(6)
f_{yp1}	Ligand production rate by S1	0.1	d^{-1}	(6)
f_{yp2}	Ligand production rate by S2	0.1	d^{-1}	(6)
f_{yls}	Strong ligand remineralization rate	0.03	d^{-1}	(6)
f_{ylw}	Weak ligand remineralization rate	0.00001	d^{-1}	(6)
f_{yd1}	Ligand release rate from detritus	0.01	d^{-1}	(6)
k_{fe_s1}	Fe half saturation for S1	0.2	$\mu mol\ m^{-3}$	(6)
k_{fe_s2}	Fe half saturation for S2	0.4	$\mu mol\ m^{-3}$	(6)

- (1) Chai F, Dugdale RC, Peng, TH, Wilkerson, FP, Barber, RT (2002) One-dimensional ecosystem model of the equatorial Pacific upwelling system. Part I: model development and silicon and nitrogen cycle. Deep Sea Res 2 Top Stud Oceanogr 49(13–14): 2713–2745.
[https://doi.org/10.1016/S0967-0645\(02\)00055-3](https://doi.org/10.1016/S0967-0645(02)00055-3)
- (2) Fujii M, Nojiri Y, Yamanaka Y, Kishi MJ (2002) A one-dimensional ecosystem model applied to time-series Station KNOT. Deep Sea Res 2 Top Stud Oceanogr 49(24–25): 5441–5461.
[https://doi.org/10.1016/S0967-0645\(02\)00207-2](https://doi.org/10.1016/S0967-0645(02)00207-2)
- (3) Fujii M, Yamanaka Y, Nojiri Y, Kishi MJ, Chai F (2007) Comparison of seasonal characteristics in biogeochemistry among the subarctic North Pacific stations described with a NEMURO-based marine ecosystem model. Ecol Model 202(1–2): 52–67.
<https://doi.org/10.1016/j.ecolmodel.2006.02.046>
- (4) Ma W, Xiu P, Chai F, Li H (2019) Seasonal variability of the carbon export in the central South China Sea. Ocean Dyn 69(8): 9552–966.
- (5) Peña MA (2003) Modelling the response of the planktonic food web to iron fertilization and warming in the NE subarctic Pacific. Prog Oceanogr 57(3–4): 453–479.
[https://doi.org/10.1016/S0079-6611\(03\)00110-1](https://doi.org/10.1016/S0079-6611(03)00110-1)
- (6) Xiu P, Chai F (2021) Impact of atmospheric deposition on carbon export to the deep ocean in the subtropical Northwest Pacific. Geophys Res Lett 48: e2020GL089640.
<https://doi.org/10.1029/2020GL089640>

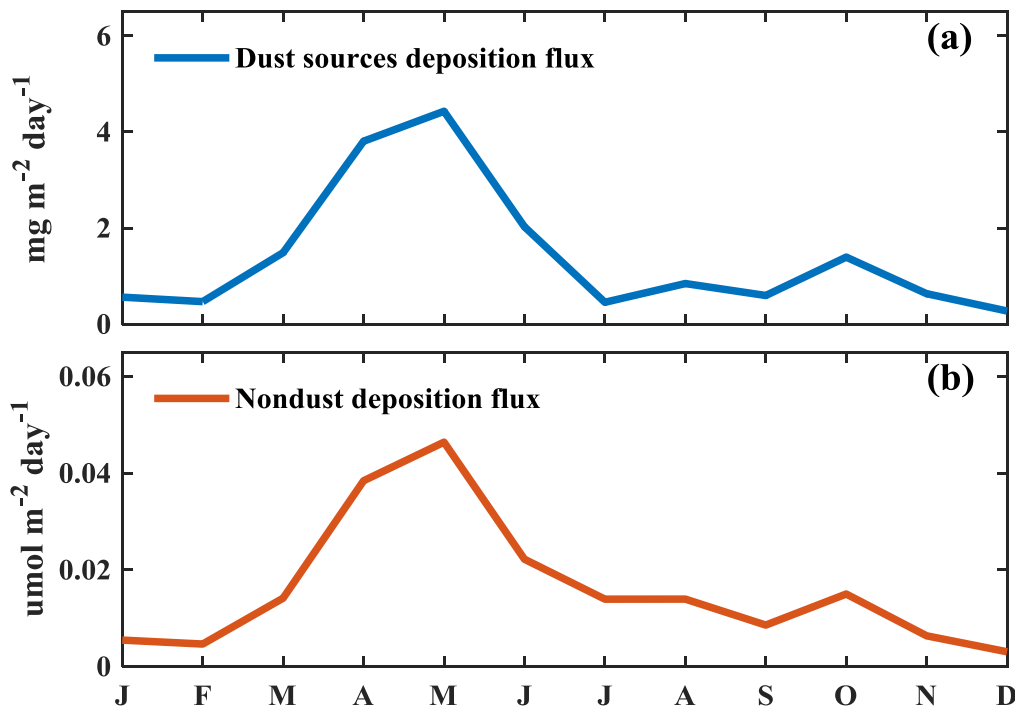


Figure S1. (a) The deposition flux of dust sources around the Papa Station, (b) nondust sources around the Papa Station

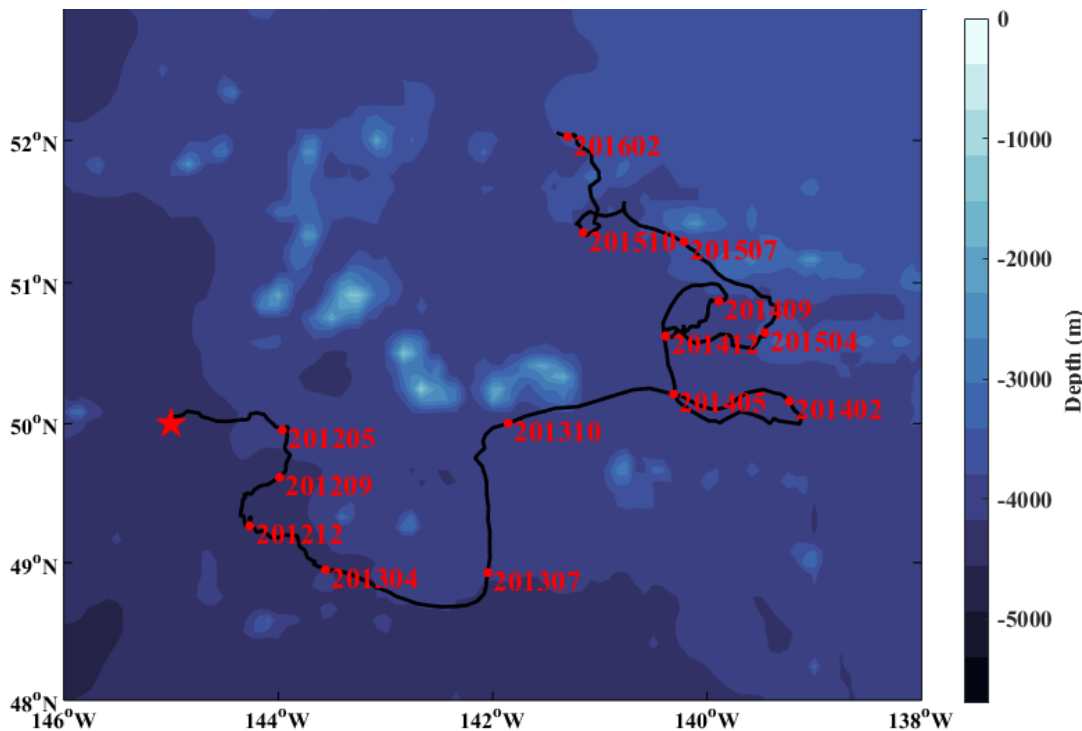


Figure S2. The float trajectory of APEX float-7601 with the location of deployment indicated as a star sign on the map. The color shading represents topography.

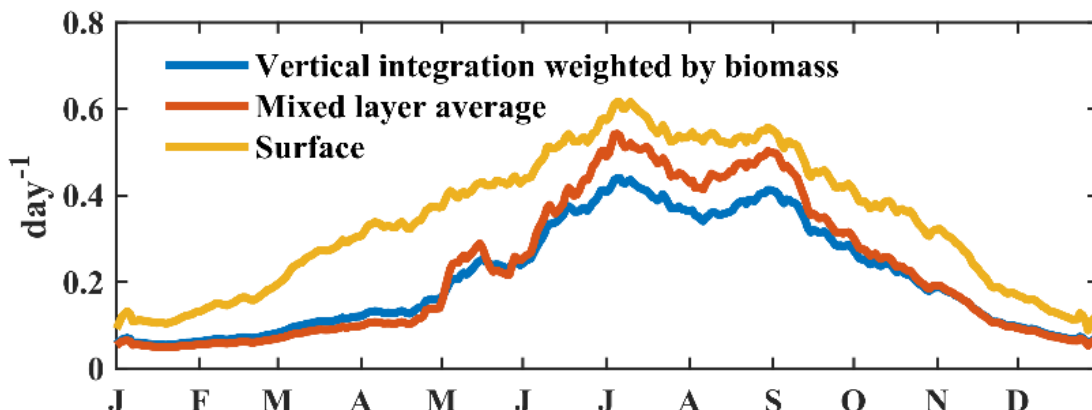


Figure S3. Modeled time series of the vertically integrated, mixed layer average and surface growth rate of small phytoplankton.

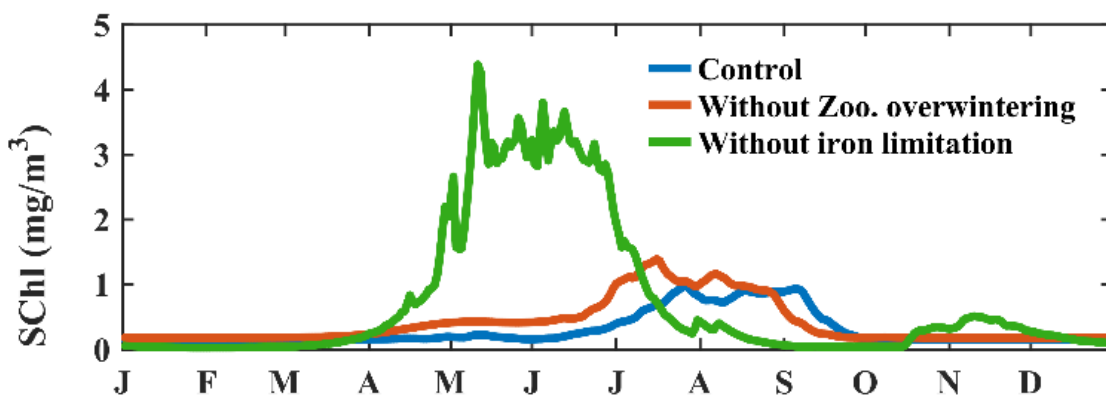


Figure S4. Modeled 1-year time series of surface chlorophyll (SChl) for the sensitivity experiments, the red solid line denotes without overwintering microzooplankton, and the green solid line denotes without Fe limitation.

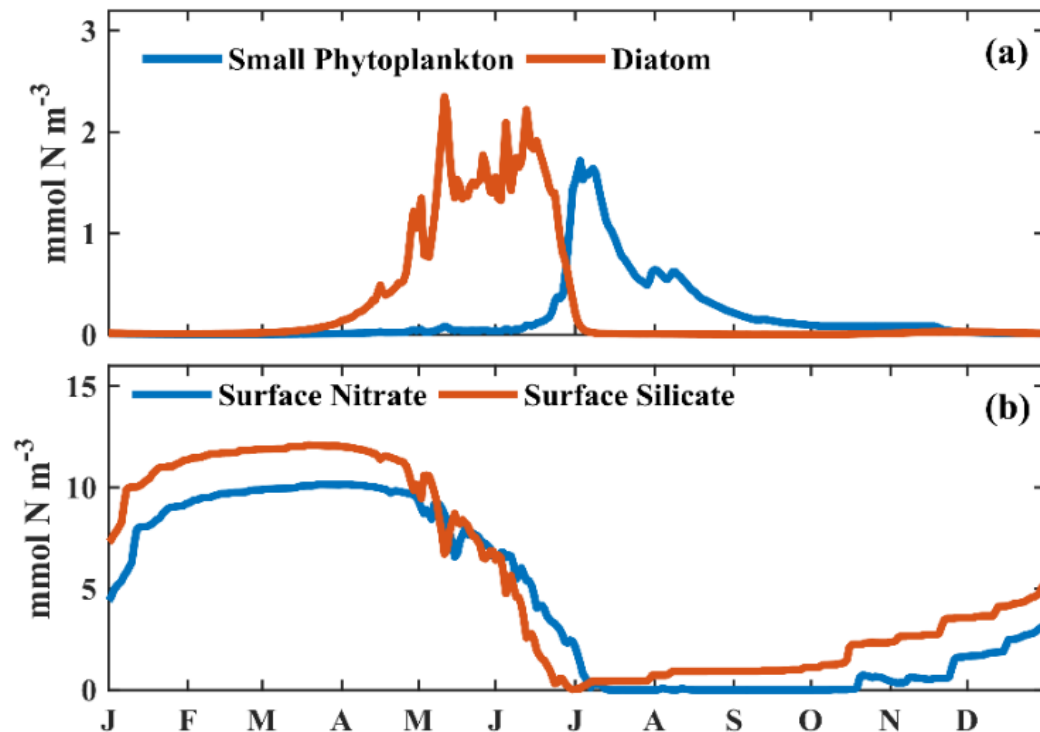


Figure S5. Modeled 1-year time series of (a) the surface small phytoplankton and diatom biomass, and (b) surface nitrate and silicate concentration for the sensitivity experiment without Fe limitation.

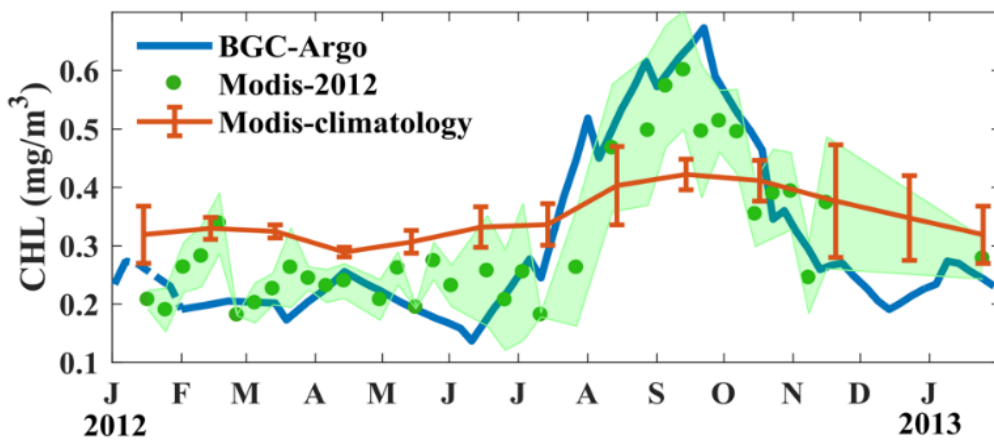


Figure S6. Comparison of MODIS 8-daily chlorophyll concentration in the sea area around Papa ($2^\circ \times 2^\circ$) in 2012 with the MODIS climatological monthly chlorophyll concentration and BGC-Argo observed surface chlorophyll concentration in 2012.

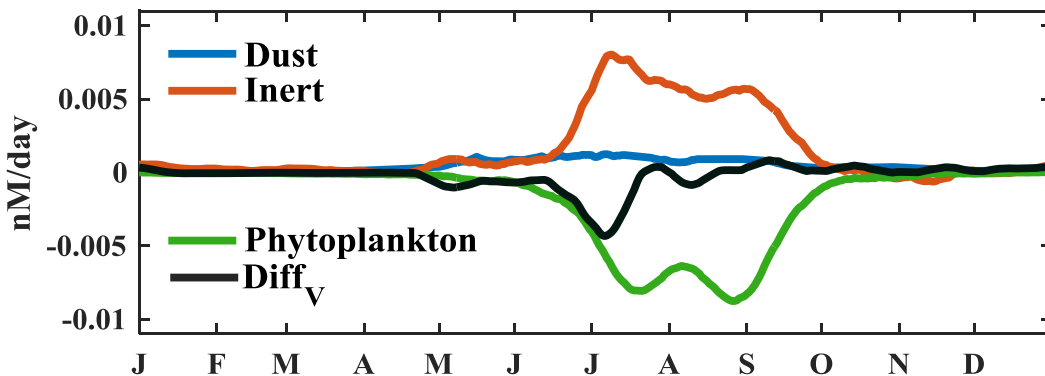


Figure S7. Modeled average net flux of each source/loss of bioavailable Fe within the mixed layer.

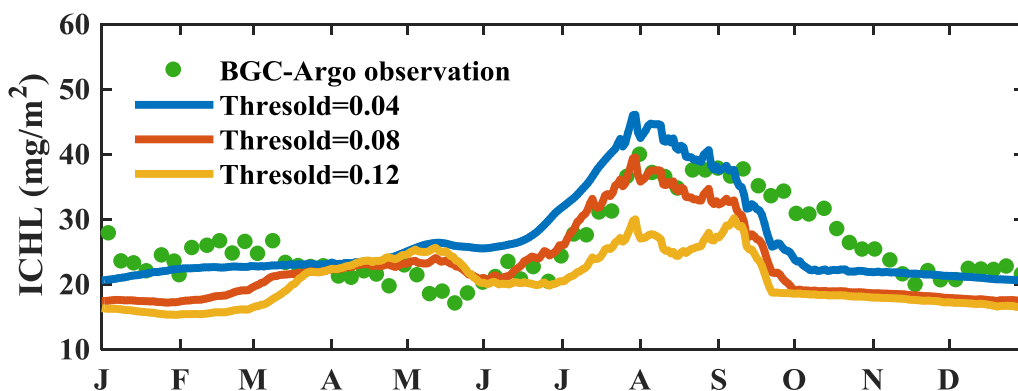


Figure S8. The depth-integrated (0–200 m) Chl-a responses of the 1D model to changes in the threshold value of mesozooplankton grazing. The green symbols denote the BGC-Argo observations.